Scanning tunneling spectroscopy of the Fe(001)-$p(1\times1)$O surface

F. Donati,[1] P. Sessi,[2] S. Achilli,[3] A. Li Bassi,[1] M. Passoni,[1] C. S. Casari,[1] C. E. Bottani,[1] A. Brambilla,[2] A. Picone,[2] M. Finazzi,[2] L. Duò,[2] M. I. Trioni,[4] and F. Ciccacci[2]

[1]*CNISM, NEMAS, and Dipartimento di Energia, Politecnico di Milano, Via Ponzio 34/3, I-20133 Milano, Italy*

[2]*CNISM, NEMAS, and Dipartimento di Fisica, Politecnico di Milano, Piazza Leonardo da Vinci 32, I-20133 Milano, Italy*

[3]*Dipartimento di Scienza dei Materiali, Università di Milano-Bicocca, Via Cozzi 53, 20125 Milano, Italy*

[4]*CNR-INFM, UdR Milano-Bicocca, Via Cozzi 53, 20125 Milano, Italy*

(Received 30 January 2009; published 21 May 2009)

In this work the density of states close to the Fermi level E_F of the Fe(001)-$p(1\times1)$O surface is investigated, by means of scanning tunneling spectroscopy (STS). STS spectra are dominated by two features, located at about 0.5 eV below E_F and 0.9 eV above E_F. The comparison with *ab initio* density-functional theory simulations of the surface electronic structure shows a very good agreement and allows assigning the observed features to minority states of the sample surface.

DOI: 10.1103/PhysRevB.79.195430 PACS number(s): 73.20.At, 68.37.Ef, 71.15.Mb

I. INTRODUCTION

The effect of oxygen adsorption on top of metal surfaces is a widely investigated topic in surface science. The understanding of the modifications in the crystallographic and electronic structure due to the presence of the adsorbate can improve the basic knowledge about fundamental processes such as oxidation, passivation, catalysis, and corrosion.[1] The case of magnetic surfaces and thin films is particularly important because of the recent attention received by effects related to the reduced dimensionality, which play a major role in the development of new nanotechnology devices.[2] It has been shown that an adsorbate can have a strong influence on the substrate magnetization, both in terms of enhancement of the local magnetic moments and of a possible inducement of a magnetic moment in the adlayer.[3,4] Both possibilities have been demonstrated to occur for oxygen adsorbed on the Fe(001) surface, in particular when oxygen chemisorption occurs in a well-ordered phase, characterized by one oxygen atom per surface unit cell, i.e., a $p(1\times1)$ phase. Structural studies of the Fe(001)-$p(1\times1)$O surface have revealed that in this system the oxygen atoms are located in the fourfold symmetrical hollow sites of the surface, with the first Fe layer outward relaxed with respect to the bulk.[5] Calculations confirm such a picture, predicting also a relatively high enhancement (at least 10%) of the magnetic moment of the outermost Fe atoms, accompanied by a small induced moment on the oxygen atoms.[4] Numerous surface magnetism sensitive experiments (namely spin polarized photoemission,[3,6] inverse photoemission,[7,8] adsorbed current spectroscopy,[9,10] metastable de-excitation spectroscopy,[10] and second-harmonic generation[11]) have been able to support these expectations, also establishing that the coupling between the surface and the substrate is ferromagnetic, and allowing for the spin character determination of the electronic structure of the topmost atoms. Efficient new electron-spin polarimeters have been built, which exploit the large spin-dependent properties of this surface.[9,12,13]

The need for a nanometer-scale investigation of the Fe(001)-$p(1\times1)$O surface is pushed by the growing interest in nanotechnology devices based on Fe/insulator interfaces.[14,15] For example, it has been predicted that the spin polarization of the current in Fe/oxide magnetic tunnel junctions can be dramatically influenced by the presence of the oxidized surface, with respect to a clean surface, also resulting in an opposite sign of the spin polarization.[16]

In this context, an investigation of this surface with atomic or nanometer-scale resolution, as it is indeed possible by means of scanning tunneling microscopy (STM), would be of great interest. Moreover, the scanning tunneling spectroscopy (STS) technique permits to investigate the surface local density of states (LDOS) close to the Fermi level E_F, and to study the distribution of characteristic surface states with a very high spatial resolution; in this respect, the physical information that can be extracted from STS data is complementary to that obtained by photoemission spectroscopies.

In this paper, we present an STM/STS study of the Fe(001)-$p(1\times1)$O surface. The measured spectra provide information about the surface electronic density of states (DOS) and are interpreted with the aid of first-principles density-functional theory (DFT) calculations of the surface electronic structure. We show that our theoretical results are in good agreement with STS experimental data, and permit to ascertain the spin character of the observed surface states at −0.5 and +0.9 eV.

II. EXPERIMENTAL AND COMPUTATIONAL DETAILS

Clean Fe(001) is obtained by ultrahigh vacuum (UHV) deposition of a thick Fe film (>100 nm) on a MgO(001) substrate.[17] The well-ordered Fe(001)-$p(1\times1)$O structure is then obtained by exposure to 30 L of pure O_2 and flash heating at 900 K, as reported in previous papers.[7,9–11]

The STM/STS measurements have been performed using an Omicron Variable Temperature (VT)-STM in a UHV chamber connected to the preparation system. STM images have been acquired at room temperature in constant-current mode with home-made electrochemically etched W tips. STS spectra (i.e., dI/dV curves) for the investigation of the sample DOS have been acquired at room temperature, using a lock-in amplifier with a modulation amplitude of 50 mV. In

order to increase the signal-to-noise ratio, all the presented STS spectra are the result of an average over tens of acquisitions[18] at same sample-tip bias V_b (sample bias with respect to the tip) and tunneling current I_t set point, i.e., at the same tip-sample distance.

First principles calculations of the surface electronic structure are performed within the DFT, using the generalized gradient approximation (GGA) for the exchange and correlation energy functional.[19] We use the embedding code implemented by Ishida[20] to treat realistic surfaces through all-electron full-potential calculations. This Green's function based embedding scheme[21] is able to consider a system which is infinite, periodic in the surface plane but nonperiodic along the surface-normal direction z. A finite "embedded" region along z is defined requiring that the perturbation due to the surface is well screened inside. The problem is then solved in such a region only. For the clean ferromagnetic iron surface we have verified that the perturbation is quite well screened within four layers beyond the surface. In addition, also the oxygen overlayer and 11 Å of vacuum have been included in the embedded region. Generalized boundary conditions guarantee the correct behavior of the solution at both the bulk and the vacuum side. The Green's function was expanded on a linearized augmented plane waves (LAPWs) basis set using 11.6 Ry as cutoff. We set $l_{\max}=9$ for the maximum angular-momentum number of the spherical expansion inside the muffin-tins, whose radii are 1.2 and 0.85 Å for iron and oxygen, respectively. The relaxed surface atomic geometry has been taken as reported in Ref. 4. The surface Brillouin zone (SBZ) was sampled by a 18×18 regular mesh which was reduced to a set of 55 independent $k_{\|}$ points.

III. RESULTS AND DISCUSSION

A. Topography

A simulation of constant-current STM images of the Fe(001)-$p(1\times1)$O surface was performed by calculating constant density surfaces in the vacuum region near the substrate, i.e., surfaces with a constant integrated DOS in the energy interval from 0 (i.e., Fermi energy) to eV_b. We show in Fig. 1 the simulated image corresponding to $V_b=0.1$ V and in which the average distance from the surface is $\bar{z}=2$ Å.

The bright spots in Fig. 1 correspond to oxygen atoms. The image has been obtained considering a two-dimensional (2D) surface average in a circle of radius 1.2 Å in order to simulate the finite extension of the tip apex. Further simulations reveal that, for larger distances (>5–6 Å), a corrugation reversal between Fe and O occurs. In fact, due to the different decay behavior of the local wave function in vacuum, Fe atoms would be imaged as the brighter spots for large distances. In the absence of a precise knowledge of the tip-sample distance such a corrugation reversal prevents a clear attribution of the bright spots in atomically resolved STM images of the surface. From these considerations it can be concluded that Fe or O atoms can be imaged as well, depending on the details of the measurement set-point conditions.

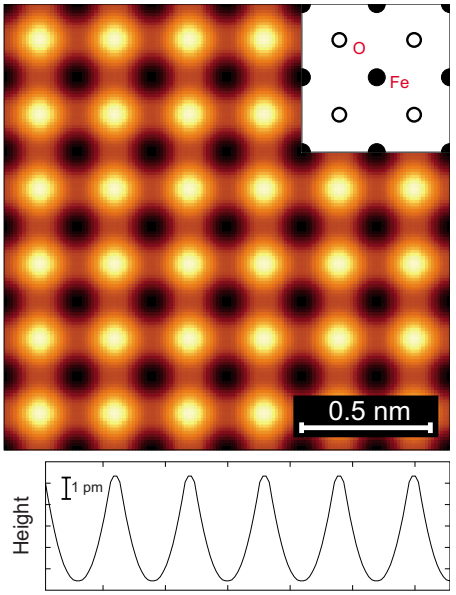

FIG. 1. (Color online) Simulated STM image of the Fe(001)-$p(1\times1)$O surface and line profile along the horizontal direction across the bright spots. Bright spots correspond to oxygen atoms.

In Fig. 2 we report a measured constant-current STM image of the Fe(001)-$p(1\times1)$O surface that clearly shows atomic resolution and the quality of the sample also at the atomic scale. In these measurement conditions we estimate the tip-sample distance to be of the order of a few Å (see Sec. III B), so that the bright spots in this image can probably be attributed to O atoms.

B. Spectroscopy

STS data have been acquired both on the clean and on the Fe(001)-$p(1\times1)$O surface. We observe that the spectral fea-

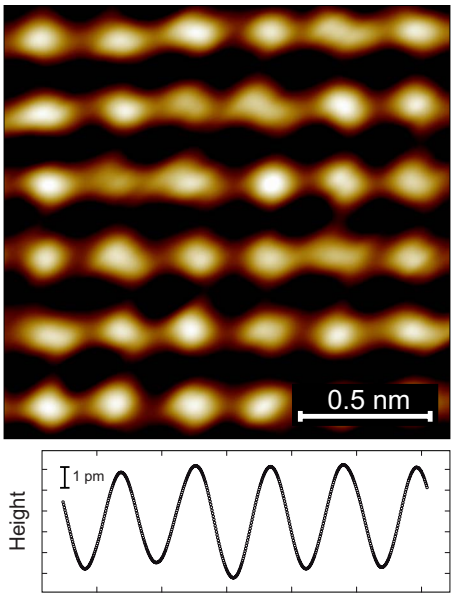

FIG. 2. (Color online) Measured constant-current STM image of the Fe(001)-$p(1\times1)$O surface and line profile along the horizontal direction across the bright spots ($V_b=160$ mV, $I_t=3.2$ nA).

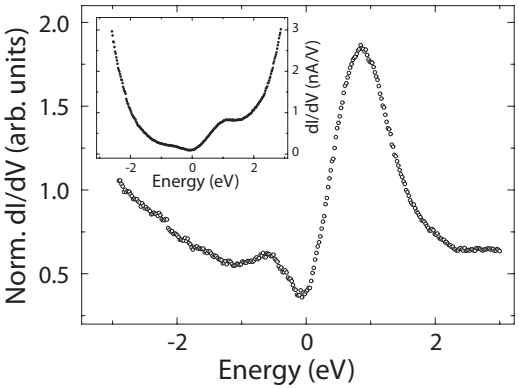

FIG. 3. Normalized STS spectrum of the Fe(001)-$p(1\times1)$O surface (measurement set-point: current I_t=0.4 nA, bias V_b=1 V). Inset: raw dI/dV experimental data.

tures that can be extracted from our measurements are independent of the lateral position of the tip with respect to the surface unit cell and consequently can be considered as average properties of the whole surface.

Prior to the analysis of the Fe(001)-$p(1\times1)$O surface, we performed an STS investigation of clean Fe(001) in order to check the surface quality before oxidation. A peak at about +0.2 eV was observed in normalized dI/dV curves, in agreement with previous measurements[22] and with our simulation (not shown).

Raw dI/dV experimental data from the Fe(001)-$p(1\times1)$O surface (inset of Fig. 3) show two features at roughly 1 eV above E_F and 0.5 eV below E_F. In order to perform a detailed analysis of the surface DOS features, thus allowing a direct comparison with *ab initio* simulations, STS curves have been analyzed using normalization to the tunneling barrier transmission coefficient T,[23] as recently discussed in Ref. 24, instead that to the experimental total conductivity I/V.[25] In the framework of a one-dimensional (1D)-Wentzel-Kramers-Brillouin (WKB) treatment of the tunneling current, it is possible to show that the following approximated expression holds:

$$\rho_t(0)\rho_s(eV) \propto \frac{dI/dV}{T_s}, \tag{1}$$

where ρ_s is the sample electron DOS at energy eV with respect to E_F, $\rho_t(0)$ is the tip electron DOS at E_F; V is the sample bias; $T_s=A[T(eV,V,z)+T(0,V,z)]$ is a symmetrical combination of the barrier transmission coefficient $T(\varepsilon,V,z)$. Using a 1D-WKB rectangular approximation, T can be written as

$$T(\varepsilon,V,z) = \exp\left[-2z\sqrt{\frac{2m}{\hbar^2}\left(\Phi+\frac{eV}{2}-\varepsilon\right)}\right], \tag{2}$$

where z is the tip-sample distance and Φ the effective work function. It can be shown that using a normalized dI/dV the sample DOS is probed mainly at positive applied voltage (unoccupied states), while the tip DOS is probed mainly at negative bias.[23] However, assuming that the tip DOS is nearly constant in the measured region, and higher than sample DOS at Fermi level, Eq. (1) gives information about both occupied and unoccupied DOS in the surface region, provided the negative bias is not too large, i.e., it can be employed to extract also features related to sample occupied states.[24] Reliable effective values of work function and tip-sample distance are required to perform this normalization. As discussed in Ref. 24, there are different possibilities to evaluate these parameters from STS data. Here we estimate the tip-sample distance by fitting the exponential tails of the dI/dV spectrum and assuming an effective work function of 4.5 eV; however, the choice of the work function does not influence the results and the discussion reported below. The tip-sample distance obtained with the fitting procedure, thus, represents an effective value to be used for the recovery of the sample DOS within a 1D description of the tunneling process and provides a rough but reasonable estimate of the real tip-sample distance.

A normalized dI/dV curve of the Fe(001)-$p(1\times1)$O surface is shown in Fig. 3. This spectrum has been measured imposing a low set-point tunneling current I_t (0.4 nA, corresponding to a relatively large tip-sample distance), so that the perturbation induced by the tip is minimized (see also Sec. III C). From the normalization procedure explained above we can estimate a tip-sample distance of about 8 Å. Two features are detected at about +0.9 and −0.5 eV. These features are always observed using different W tips and have also been measured using bulk Cr tips;[26] we can thus safely attribute them to the sample electronic structure.

In order to interpret the measured STS spectrum we studied the Fe(001)-$p(1\times1)$O surface from first principles. The number of theoretical studies is scarce; the main part of them are devoted to the structural properties of the system[4,27,28] and only few works discuss spectral properties.[3,16,29] One of the most accurate calculation has been performed by Clarke *et al.*[3] and it shows the surface band structure along a high-symmetry path of the SBZ. In their work surface states are distinguishable from the discrete features that form the projected bulk bands, on the basis of the spatial localization of the wave function in the surface region. In our embedding approach, due to the infinite extension of the substrate, the surface band structure is a continuous function of the energy for each $k_\parallel$ point of the SBZ so that surface resonances and discrete states can be easily evidenced.

The adsorption of oxygen on the iron surface leads to a partial modification of the surface electronic properties. Although the bonding p levels of oxygen lie very deep in energy, the antibonding states, which extend for some eV around the Fermi level, hybridize with the Fe surface atoms electronic structure. In Fig. 4 we report the computed surface band structure for the majority (left panel) and the minority (right panel) spin components calculated in the first Fe and O layers. The brighter regions correspond to higher density of states and narrow lines are very sharp features. The less dispersive d bands extend in the energy interval between −5 and −1 eV for the majority component and between −2 and 2 eV for the minority one. We note that due to the surface band narrowing the exchange splitting at the Fermi level is larger than in the bulk.

Surface states can be identified as the brightest lines in Fig. 4. In particular at $\bar{\Gamma}$ majority-spin surface states are

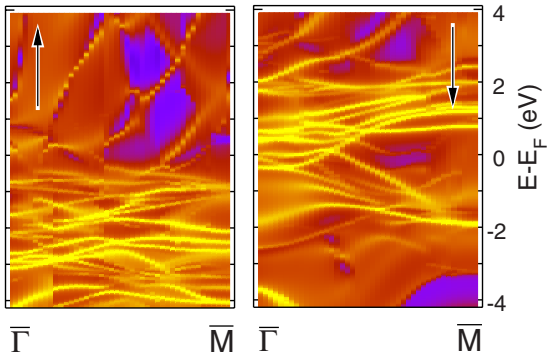

FIG. 4. (Color online) Computed surface band structure of Fe(001)-$p(1\times1)$O: majority and minority-spin components are reported in the left and right panels, respectively.

found at −3, −1.6, and −0.8 eV. On the other hand minority-spin surface features lie at higher energies, namely at −0.35 eV, in a 1 eV wide range above the Fermi level, at 1.7, and 2.1 eV.

In Fig. 5(a) we report the computed density of states evaluated in the two surface layers (Fe and O), in the energy interval proper of the STS measurements. The majority and minority components are reported in the upper and lower panels, respectively, while the dotted line corresponds to the total DOS. No evidence of adsorption induced surface-state reorganization with respect to clean Fe(001) is found in the majority component. On the other hand the minority-spin feature (found at 0.18 eV) of clean Fe(001) is not observed

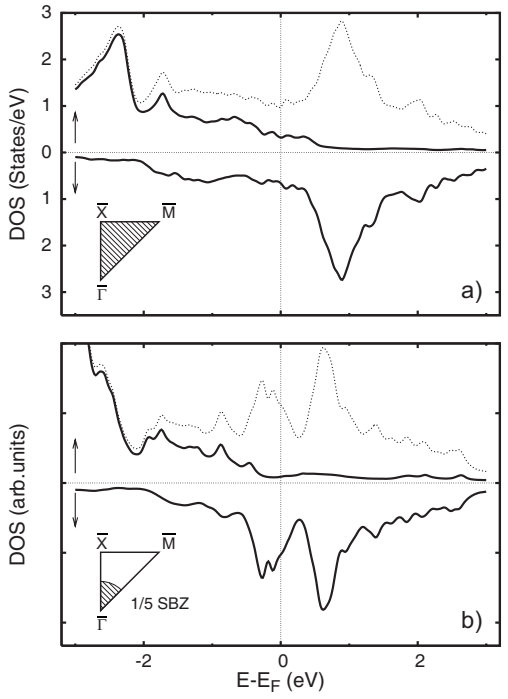

FIG. 5. (a) Computed density of states of Fe(001)-$p(1\times1)$O in the surface region (surface and subsurface layer). (b) Computed density of states of Fe(001)-$p(1\times1)$O integrated only into 1/5 of the SBZ around $\bar{\Gamma}$; upwards arrow: majority-spin component; downwards arrow: minority-spin component; dotted line: total DOS.

upon adsorption of oxygen, while a peak at 0.8 eV is found that we identify as a surface resonance due to its large amplitude in the vacuum region. We observe that the computed position of this unoccupied minority surface state is in very good agreement with the measured position of the large peak at positive bias in STS data.

A further effect of the O-Fe interaction is represented by the enhancement of the magnetization in the surface iron layer (passing from $2.97\mu_B$ of the clean surface to $3.22\mu_B$ upon the oxygen adsorption) and the appearance of a spin polarization also in the oxygen layer, which we calculated to be equal to $0.22\mu_B$, in agreement with previous findings.[4,16,27]

Due to the faster decay toward the vacuum of the wave functions at large $k_{\|}$, the STS probing method has a higher sensitivity to states around the $\bar{\Gamma}$ point.[30] This is usually the case for surface states, even though different situations can exist, since the decay in vacuum depends on the specific dispersion relation for the considered surface state. This aspect is not considered in the 1D-WKB normalization procedure of experimental data. A simple method in order to permit a qualitative but direct comparison between measured STS data and theoretical DOS, which would not be otherwise straightforward, is to integrate the latter one in a smaller region of the SBZ.[22]

Here, considering the contribution to the DOS only from 1/5 of the SBZ around $\bar{\Gamma}$, we obtain some new features with respect to the total DOS, which give account of the measured peaks. In addition to the main minority peak at +0.8 eV, structures at the Fermi level in the minority component, peaked at about −0.35 eV, appear, together with a structure at −0.9 eV in the majority component [see Fig. 5(b)]. The enhancement of the spectral weight of these structures upon integrating within a restricted region of the SBZ is due to the flat dispersion around the $\bar{\Gamma}$ point.

In this way satisfactory agreement between experiment and theory is obtained not only for the minority peak at +0.8 eV, but also for the structure at negative energy (−0.35 eV from theory vs −0.5 eV from experiments). The agreement is even better if effects related to measurement conditions are taken into account, as discussed in next section. *Ab initio* calculations indicate the minority-spin character of the measured surface states. We observe that the broadening of the measured features with respect to calculations could be related to a convolution of the fine structures visible in Fig. 5.

C. Influence of measurement conditions

We have already mentioned that minimizing the tunneling current and the tip electric field (i.e., at large tip-sample distance) corresponds to a situation which is closer to the unperturbed isolated surface (in equilibrium). When a larger set-point tunneling current is employed for STS measurements, and the corresponding tip-sample distance is decreased, leading to a significant perturbation of the system, a shift of the above discussed peaks is observed.

In Fig. 6 we show normalized dI/dV data from the Fe(001)-$p(1\times1)$O surface, acquired using different $I_t - V_b$

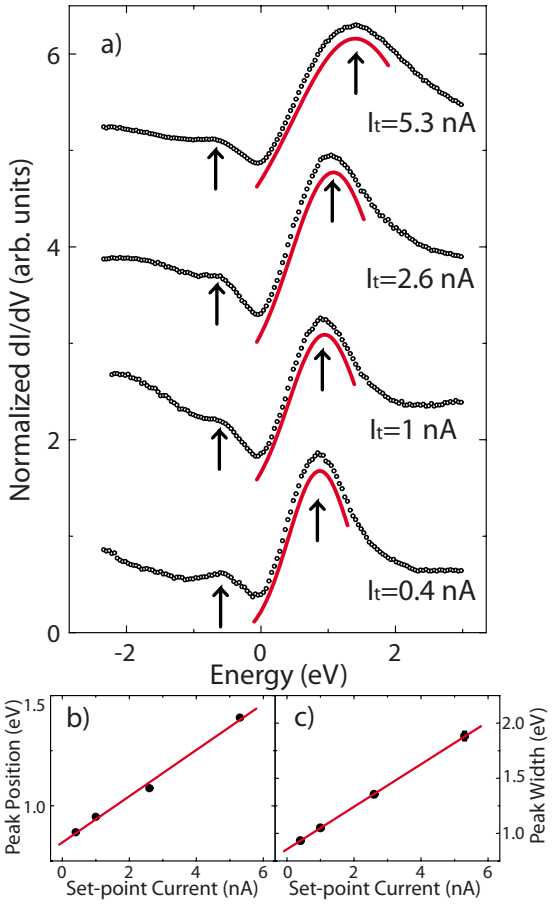

FIG. 6. (Color online). (a) Normalized STS spectra of the Fe(001)-$p(1\times1)$O surface, measured at different values of the set-point current I_t (V_b=1 V). The arrows indicate the energy positions of the surface states; Gaussian fit for the feature in unoccupied states is shown (solid line). (b) Position and (c) width of the peak in the unoccupied states as a function of set-point current I_t. Linear fit is shown (solid line).

set points (in particular different set-point current in the range from 0.4 to 5.3 nA, keeping the set-point bias at 1 V). The same two features commented above are detected; nevertheless both peaks broaden and shift away from the Fermi level when increasing the tunneling current I_t. This observation is not affected by the normalization procedure, i.e., the same trend as a function of set-point can be detected in raw (i.e., non-normalized) dI/dV data (not shown).

In order to quantitatively evaluate these effects, we performed a Gaussian fit of the large feature. Both position and width increase linearly when increasing I_t, as shown in Fig. 6. From the linear fit, we can extrapolate the peak position E_0 and the full width at half maximum (FWHM) w_0 at zero current, and we obtain E_0=0.83 eV and w_0=0.85 eV. A similar effect (shift to more negative bias) is qualitatively observed for the peak in the occupied states, even though much less marked (and difficult to quantify, since the feature is weak and not easily separable from the background). We note that this kind of effect is not observed on the clean Fe(001) surface [i.e., the position of the peak at +0.2 V is not influenced by the tunneling current (see e.g., Ref. 22)]. Also, the large shift detected when the set-point current increases from 2.6 to 5.3 nA corresponds to a very small difference in tip-sample distance (a reasonable estimate provides $\Delta z < 0.5$ Å).

Different effects have been invoked in the literature to explain observed shifts of STS features as a function of the measurement set point, i.e., of the applied electric field between tip and sample and/or of the tunneling current, for instance tip-induced band bending (in semiconducting surfaces),[31] Stark effect,[32] different decay behavior of surface wave functions into vacuum,[33] and transport-limited surface charging (i.e., setup of a nonequilibrium surface configuration, in which one or more electrons are injected into unoccupied surface states).[34,35]

Even though no definite conclusion can be drawn in our case yet, simple arguments point toward a reduction in possible candidates. In fact band bending effects are typical of semiconductors, being electric field effects in metal surfaces usually much smaller. Also, the large shift detected upon a small change in tip-sample distance (i.e., going from 2.6 to 5.3 nA set-point current) points into the direction of excluding effects related to the tip electric field perturbing the system, or to the different decay behavior of surface wave functions into vacuum.

Within this simple scheme, an out-of-equilibrium configuration due to electron injection in the surface seems to be the major responsible for the observed shift. In this context, we note that the situation for STS is qualitatively similar to inverse photoemission spectroscopy (IPS), in which electrons are also added to the system. In particular, IPS data from Fe(001)-$p(1\times1)$O identify a surface feature (located at 1.8 eV above E_F) that is shifted to larger energy with respect to theoretical expectations.[8] In that case, the discrepancy has been attributed to the difference between the excited states in the presence of an extra electron (sampled in IPS) as compared to those calculated for the unperturbed system. This difference can originate sizable shifts of the spectral features toward higher energies in experiments in which electrons are added to a system with low screening efficiency. This is actually the case for Fe-O systems where oxygen atoms act as ligands with considerably localized states, as it has been thoroughly discussed for bulk FeO.[36] Similar effects could well be at the basis of the present STS findings when the tunneling current injected into the surface is increased. A deeper understanding of the observed shifts would of course benefit from simulations of the surface in out-of-equilibrium conditions or in the presence of a strong localized electric field.

However, we can conclude that good agreement is obtained if the zero-current extrapolated position E_0=0.83 eV is directly compared to the computed energy position of the surface state (0.83 vs 0.8 eV). Physically, we can interpret this limit as corresponding to infinite tip-sample distance, i.e., unperturbed system.

IV. CONCLUSIONS

We have investigated the local density of states close to the Fermi level of the Fe(001)-$p(1\times1)$O surface, by means of STS and *ab initio* simulations of the surface electronic

structure based on DFT in GGA approximation. The STS spectra show two peaks, at about 0.5 eV below E_F and 0.9 eV above E_F, respectively. *Ab initio* computations provide a good agreement with measured positions, and permit to interpret the observed features as related to minority surface states. In particular when oxygen is adsorbed on the clean Fe(001) surface a strong surface resonance at 0.8 eV is found. STS measurements at low set-point currents provide a DOS measurement which can be directly compared to the unperturbed equilibrium surface situation and a value of 0.83 eV is thus retrieved, very close to the theoretical one.

The study of the local magnetic properties of this surface by the spin polarized-STM/STS technique,[37] based on the use of magnetic tips, looks promising for a complete understanding of the spin character of the observed surface states, already unveiled by our *ab initio* calculations.

ACKNOWLEDGMENTS

NEMAS (Center for NanoEngineered MAterials and Surfaces) is a center of excellence of the Italian Ministry for University and Research (MIUR) located at Politecnico di Milano. This work has partially been funded by MIUR through PRIN Project No. 2007CMLFY2.

[1] G. A. Somorjai, *Introduction to Surface Chemistry and Catalysis* (Wiley, New York, 1994).
[2] C. A. F. Vaz, J. A. C. Bland, and G. Lauhoff, Rep. Prog. Phys. **71**, 056501 (2008).
[3] A. Clarke, N. B. Brookes, P. D. Johnson, M. Weinert, B. Sinković, and N. V. Smith, Phys. Rev. B **41**, 9659 (1990).
[4] S. R. Chubb and W. E. Pickett, Phys. Rev. Lett. **58**, 1248 (1987).
[5] K. O. Legg, F. Jona, D. W. Jepsen, and P. M. Marcus, Phys. Rev. B **16**, 5271 (1977).
[6] P. D. Johnson, A. Clarke, N. B. Brookes, S. L. Hulbert, B. Sinković, and N. V. Smith, Phys. Rev. Lett. **61**, 2257 (1988).
[7] R. Bertacco and F. Ciccacci, Phys. Rev. B **59**, 4207 (1999).
[8] S. De Rossi, L. Duò, and F. Ciccacci, Europhys. Lett. **32**, 687 (1995).
[9] R. Bertacco, M. Merano, and F. Ciccacci, Appl. Phys. Lett. **72**, 2050 (1998).
[10] F. Bisio, R. Moroni, M. Canepa, L. Mattera, R. Bertacco, and F. Ciccacci, Phys. Rev. Lett. **83**, 4868 (1999).
[11] M. Nyvlt, F. Bisio, J. Franta, C. L. Gao, H. Petek, and J. Kirschner, Phys. Rev. Lett. **95**, 127201 (2005).
[12] R. Bertacco, M. Marcon, G. Trezzi, L. Duò, and F. Ciccacci, Rev. Sci. Instrum. **73**, 3867 (2002).
[13] A. Winkelmann, H. Hartung, D. Engelhard, C.-T. Chiang, and J. Kirschner, Rev. Sci. Instrum. **79**, 083303 (2008).
[14] M. Finazzi, L. Duò, and F. Ciccacci, Surf. Sci. Rep. **64**, 139 (2009).
[15] N. Rougemaille, M. Portalupi, A. Brambilla, P. Biagioni, A. Lanzara, M. Finazzi, A. K. Schmid, and L. Duò, Phys. Rev. B **76**, 214425 (2007).
[16] E. Yu. Tsymbal, I. I. Oleinik, and D. G. Pettifor, J. Appl. Phys. **87**, 5230 (2000).
[17] R. Bertacco, S. De Rossi, and F. Ciccacci, J. Vac. Sci. Technol. A **16**, 2277 (1998).
[18] A small component of noise affects the amplitude of every single measure but the variance on the dI/dV value remains below the 15% of the total signal dynamics at every applied bias. The position and the shape of the main spectroscopic features discussed in this work are not affected by this kind of noise.
[19] J. P. Perdew, K. Burke, and M. Ernzerhof, Phys. Rev. Lett. **77**, 3865 (1996).
[20] H. Ishida, Phys. Rev. B **63**, 165409 (2001).
[21] J. E. Inglesfield, J. Phys. C **14**, 3795 (1981).
[22] J. A. Stroscio, D. T. Pierce, A. Davies, R. J. Celotta, and M. Weinert, Phys. Rev. Lett. **75**, 2960 (1995).
[23] V. A. Ukraintsev, Phys. Rev. B **53**, 11176 (1996).
[24] M. Passoni, F. Donati, A. Li Bassi, C. S. Casari, and C. E. Bottani, Phys. Rev. B **79**, 045404 (2009).
[25] J. A. Stroscio, R. M. Feenstra, and A. P. Fein, Phys. Rev. Lett. **58**, 1668 (1987).
[26] A. Li Bassi *et al.*, Appl. Phys. Lett. **91**, 173120 (2007).
[27] P. Bloński, A. Kiejna, and J. Hafner, Surf. Sci. **590**, 88 (2005).
[28] P. Bloński, A. Kiejna, and J. Hafner, J. Phys.: Condens. Matter **19**, 096011 (2007).
[29] C. M. Fang, R. A. de Groot, M. M. J. Bischoff, and H. van Kempen, Surf. Sci. **445**, 123 (2000).
[30] M. Passoni and C. E. Bottani, Phys. Rev. B **76**, 115404 (2007).
[31] R. M. Feenstra, G. Meyer, and K.-H. Rieder, Phys. Rev. B **69**, 081309(R) (2004).
[32] L. Limot, T. Maroutian, P. Johansson, and R. Berndt, Phys. Rev. Lett. **91**, 196801 (2003).
[33] W. A. Hofer, J. Redinger, A. Biedermann, and P. Varga, Surf. Sci. **482-485**, 1113 (2001).
[34] R. M. Feenstra, S. Gaan, G. Meyer, and K.-H. Rieder, Phys. Rev. B **71**, 125316 (2005).
[35] J. Mysliveček, A. Stróżecka, J. Steffl, P. Sobotík, I. Ošt'ádal, and B. Voigtländer, Phys. Rev. B **73**, 161302(R) (2006).
[36] L. Braicovich, F. Ciccacci, E. Puppin, A. Svane, and O. Gunnarsson, Phys. Rev. B **46**, 12165 (1992).
[37] M. Bode, Rep. Prog. Phys. **66**, 523 (2003).